Asymptotic Theory of Propeller Noise Part II: Supersonic Single-Rotation Propeller

D. G. Crighton*
University of Cambridge, Cambridge, England CB3 9EW, United Kingdom
and
A. B. Parry†
University of Strathclyde, Glasgow, Scotland G1 1XH, United Kingdom

This paper gives analytical formulas for the far-field harmonic components of the acoustic radiation from a B-bladed supersonic single-rotation propeller, in the asymptotic limit $B \to \infty$. The dominant source, for radiation in a given direction, is identified as located at the Mach radius along the blade span, the radius that approaches the observer at precisely sonic speed, once in each rotation. Favorable agreement is found between the asymptotic prediction and the results of full numerical evaluation of the radiation integrals. Singular surfaces in the field are identified from the asymptotic formulas, which are extended to include chordwise noncompactness effects. These show, among other things, that supersonic propeller noise is an algebraically decreasing function of tip Mach number, once chordwise noncompactness effects are taken into account, in contrast to the exponential increase with tip Mach number of subsonic propeller noise.

Nomenclature

B = number of blades
b = airfoil maximum thickness
C_L = lift coefficient
c = airfoil chord
c_0 = speed of sound
D = propeller diameter
$F(X)$ = normalized loading distribution
$H(X)$ = Heaviside step function
$h(X)$ = normalized thickness distribution
J_{mB} = Bessel function of first kind and of order mB
k_x = chordwise wave number, $2mB(c/D)M_t/(1 - M_x \cos\theta)M_r$
k_y = wave number normal to chord, $2mB(c/D)(M_r^2 \cos\theta - M_x)/(1 - M_x \cos\theta)zM_r$
M_r = section relative Mach number
M_t = tip rotational Mach number
M_x = flight Mach number
$M_0(\theta)$ = tip Mach number component in direction θ
m = harmonic index
P_m = normalized harmonic pressure coefficient
p = acoustic pressure
r_0 = hub-observer separation at emission time
$S(z)$ = normalized source strength, see Eqs. (3) and (4)
t = observer time
X = normalized chordwise coordinate
$\mathbf{x}$ = observer location
z = normalized spanwise coordinate
z^* = Mach radius, defined by Eq. (7)
z_0 = normalized hub radius
α_L, α_T = coefficients of loading or thickness distribution at leading (L) and trailing (T) edge
θ = radiation angle (at emission time) from propeller axis to observer
λ = $\sec^{-1}(z/z^*)$, see Eq. (9)
ν_L, ν_T = exponents of loading or thickness distribution at leading (L) and trailing (T) edge
ρ = fluid density
τ = retarded time, $t - r_0/c_0$
ϕ_s = phase associated with blade sweep ($\phi_s = 0$ throughout this paper)
Ψ_L, Ψ_V = chordwise noncompactness factors associated with blade loading and thickness, respectively; see Eqs. (5) and (6)
ψ_0 = circumferential angle from observer to reference location, see Fig. 1
Ω = shaft angular speed

Received Nov. 20, 1989; revision received Jan. 10, 1991; accepted for publication Jan. 15, 1991. Copyright © 1991 by the American Institute of Aeronautics and Astronautics, Inc. All rights reserved.

*Professor of Applied Mathematics, Department of Applied Mathematics and Theoretical Physics, Silver Street. Member AIAA.
†Lecturer in Industrial Mathematics, Centre for Industrial Mathematics and Control.

I. Introduction

In Part I of this paper, the authors[1] gave a prediction scheme for the steady loading and thickness components of the far-field noise of a subsonic single-rotation propeller. The scheme was based on the asymptotic evaluation of the radiation integrals, with specified distributions of loading and thickness, in the general frequency-domain formulation of Hanson.[2] The large parameter underlying the asymptotic approximations was taken as the number of blades B, so that the approximation in mind is that of the "many-bladed propeller" but with this understood to imply no more than the formal limit $B \to \infty$. Since it is actually the product mB of harmonic number and blade number that always appears, one could alternatively think of the limiting behavior as achieved in the high-frequency limit, corresponding to $m \to \infty$. However, low-order harmonics are of some importance also, and it is preferable to regard B as large, with m taking all integer values, although naturally the asymptotic behavior for a propeller with *given* B agrees increasingly closely with full numerical evaluation of the radiation integrals as m increases. The results of Part I were found to be represented by a number of simple analytical formulas giving in explicit terms the dependence of the far-field sound on observation angle θ, on axial and tip rotational Mach numbers M_x and M_t, on the product mB, and, most crucially, on only the distributions of loading and thickness close to the blade tip. In this sense, subsonic propeller noise is tip generated, and the contributions of all inboard blade sections are exponentially weaker than those from the tip, when $mB \gg 1$. Effects of chordwise

noncompactness and of blade sweep were also accounted for in simple results asymptotically valid for large mB.

This paper goes on to the corresponding analysis for a supersonic single-rotation propeller. Several treatments of this problem have been given, both in the time domain[3-5] and in the frequency domain,[2,6,7] and there are indeed treatments that have some overlap with our approach. Specifically, Hawkings and Lowson,[8] considering a propeller with supersonic rotational speed and zero axial velocity, point out the separation of the propeller disk into an inner circle, all of whose points have subsonic velocity toward a given observer, and an outer annulus, all of whose points at some time in each revolution approach that observer supersonically. The boundary is, for an observer in the plane of the propeller ($\theta = \pi/2$) and for $M_x = 0$, just the radius at which the local (rotational) Mach number is unity. This might lead one to call the boundary in the general case ($M_x \neq 0$, $\theta \neq \pi/2$) the "sonic radius," i.e., that radius at which the blade element at some point in each revolution approaches the observer with precisely sonic speed. That leads, however, to confusion because the region around that radius is not in general one of transonic aerodynamics in the usual sense of relative Mach number close to unity, and of course that radius is a strong function of observer angle θ. Here we shall give it the name "Mach radius" and emphasize its dependence on θ, M_x, and M_t. Although Hawkings and Lowson correctly identified the qualitative characteristics of radiation from the regions inboard and outboard of the Mach radius, they did not, however, fully exploit the limit $mB >> 1$ as we shall do here to produce simple explicit formulas describing—at leading order—the dominant radiation from the Mach radius and—at the next order—from the blade tip.

Now the harmonic amplitudes of subsonic propeller noise decay exponentially[1] as $|m| \to \infty$. Accordingly, the waveform $p(\mathbf{x},t)$ is infinitely differentiable as a function of t, for all $\mathbf{x}$. By contrast, the harmonic amplitudes generated by the blade region around and outboard of the Mach radius decay only as some inverse power of $|m|$, so that there are singular surfaces in the field on which p itself, or derivatives of p, will have singularities. These focusing singularities have been noted before; they are implicit in the formulation of Ffowcs Williams and Hawkings[9] and were analyzed in some detail for thickness noise by Tam[10] and, more recently and in much more detail, by Chapman,[11] Amiet,[12] and Lindblad.[6] We do not draw particular attention to them, as we are interested in the whole field, not just in the focusing singularities, whose origin has been very clearly explained by the authors mentioned. We do, however, stress that they emerge completely naturally from our frequency-domain approach, and we indicate very briefly the essential nature of the singularity for the *general* case, covering both loading and thickness noise and all possible distributions of loading and thickness near the blade leading edges (which control the strength of the singularities), and allowing for axial and rotational motion; no such full picture has been given elsewhere, and it would be straightforward from our results to supply all details of this focusing phenomenon, at any rate within linear theory.

We begin Sec. II with some definitions and notation, then continue with a derivation of results illustrating the fundamental "Mach radius" mechanism for supersonic propeller noise. This section includes a comparison of those analytical results with full numerical computation, and a brief examination of singularities in the far-field pressure, and it also describes a first approximation to chordwise noncompactness effects. These latter are not nearly so simple to deal with as in the subsonic case, for in the supersonic case there is already significant phase cancellation in the region outboard of the Mach radius in the compact-chord limit, so that noncompactness gives rise to a competition between two processes of rapid cancellation. Effects of blade sweep are similar and can and should be dealt with at the same time, and so many new effects are introduced that we have decided to deal with all such issues fully in a separate paper. Nonetheless, the simple approach to chordwise noncompactness leads to some significant results, among them the prediction that at supersonic speeds the harmonic amplitudes of the far-field sound decrease algebraically as the tip Mach number increases, in marked contrast to the exponential increase with tip Mach number that occurs at subsonic speeds.

Section III contains concluding remarks, and the Appendix has brief notes on the relation between the harmonic series in the frequency domain and the singular pressure in the time domain.

II. Basic Mechanism of Supersonic Propeller Noise

Definitions

For an observer at rest in static, ambient fluid, the pressure generated by a propeller with axial and rotational motion is time harmonic in the far-field approximation, and Hanson[2] has given expressions of the form

$$P_m = \int_{z_0}^{1} S(z) J_{mB}\left(\frac{mBM_t z \sin\theta}{1 - M_x \cos\theta}\right) dz \tag{1}$$

for the far-field harmonic components P_m of the radiated pressure from a B-bladed propeller. A factor

$$-\frac{\rho c_0^2 DB}{8\pi r_0(1 - M_x\cos\theta)} \exp\left[\frac{imB\Omega}{(1 - M_x\cos\theta)}\left(t - \frac{r_0}{c_0}\right) + imB\left(\frac{\pi}{2} - \psi_0\right)\right] \tag{2}$$

has been removed from the P_m, and the source terms $S(z)$ corresponding to blade loading and blade thickness are given, respectively, by

$$S(z) = M_r^2 e^{-i\Phi_s}\left(ik_y \frac{C_L}{2}\right)\Psi_L(k_x) \tag{3}$$

$$S(z) = M_r^2 e^{-i\Phi_s}\left(k_x^2 \frac{b}{c}\right)\Psi_V(k_x) \tag{4}$$

(Quadrupole effects are neglected, except in so far as they contribute to the steady loading distribution, which is assumed given.) The notation and symbols are defined in the Nomenclature and in Fig. 1. We draw attention to the definition of z as a normalized spanwise coordinate ($z = z_0$ the blade hub, $z = 1$ the tip) and X as a normalized chordwise coordinate, $X = \mp\frac{1}{2}$ corresponding to the leading and trailing edges,

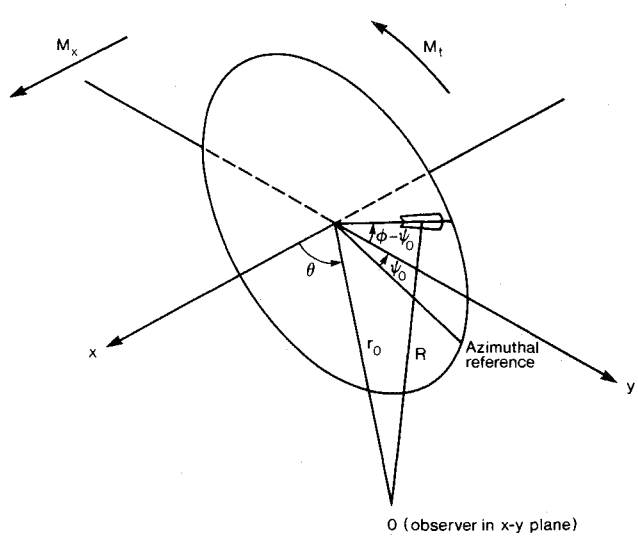

Fig. 1 Propeller geometry in the nominal disk plane.

respectively. The chordwise noncompactness factors appearing in Eqs. (3) and (4) are defined by

$$\Psi_L(k_x) = \int_{-1/2}^{1/2} F(X) \exp(-ik_x X)\, dX \tag{5}$$

$$\Psi_V(k_x) = \int_{-1/2}^{1/2} h(X) \exp(-ik_x X)\, dX \tag{6}$$

where $F(X)$ and $h(X)$ are normalized loading and thickness distributions across the chord. The normalization is such that in the compact-chord limit $k_x \to 0$, we have $\Psi_L = \Psi_V = 1$.

For subsonic relative tip Mach numbers and for thin blades, the adequacy of Eqs. (1–4) (with careful numerical evaluation, using as input the known thickness distribution and the loading distribution obtained from standard aerodynamic codes) has been demonstrated many times in comparison with experimental data. Whether that remains the case with supersonic blades is less clear, and the possible role of quadrupole sources supplementing those in Eqs. (3) and (4) remains open, although a commonly held view, with some theoretical backing, is that such quadrupole sources are unimportant for sufficiently thin blades. We shall deal here only with the thickness and loading sources, and our aim is to expose the physical mechanisms underlying Eq. (1) and to provide simple approximate formulas that reproduce the exact numerical evaluation of Eq. (1) with acceptable accuracy. Our asymptotic method is, however, perfectly well adapted to the evaluation of the quadrupole integral also, should that be shown by later work to be necessary.

We shall study Eq. (1) in the asymptotic limit, $B \to \infty$, of the many-bladed propeller. This will actually cover all harmonic components, $m = \pm 1, \ldots$, since $|mB| >> 1$ is what is needed for the asymptotics (and $m = 0$ is trivial for the single-rotation propeller, although not for the counterrotation propeller, where $m = 0$ needs separate analysis). Part I of this paper showed that this was an effective procedure for subsonic conditions, where it led to a proof that the radiation was tip dominated (with exponentially small relative errors) and to simple formulas for the radiation that gave excellent agreement with the results of full numerical evaluation (except for tip conditions approaching sonic, where a different asymptotic description is needed and will be given in a companion paper). We shall be able to make comparable claims for the corresponding analysis here of the supersonic case, except that the errors are now algebraically small, rather than exponentially, implying that a rather higher value of mB will be needed for a given accuracy. However, the dominant radiation mechanism is now quite different, arising, as has been pointed out before from a variety of different approaches,[8,9] from sonic motion of a blade section toward a given observer.

Mach Radius

When the propeller blade tips are operating supersonically, the tip Mach number component $M_0(\theta) = M_t \sin\theta + M_x \cos\theta$ can be greater than unity for θ within a certain range. For each θ in that range there is a section of the blade, $z = z^*$, that approaches the observer at θ with precisely sonic speed. This section is defined by

$$1 = z^* M_t \sin\theta + M_x \cos\theta \tag{7}$$

We refer to z^* as the "Mach radius" and emphasize the dependence of z^* on θ. In this case, the blade tips are no longer the most efficient radiators of sound since, for large values of mB, the radiation efficiency, represented by the Bessel function in Eq. (1), peaks near the radial station defined by Eq. (7).

For the present we neglect the effects of chordwise noncompactness, setting the factors Ψ_L and Ψ_V equal to unity (and we have already said that blade sweep effects will be ignored throughout this paper), so that the harmonic components of the radiated sound are given by

$$P_m = \int_{z_0}^{1} S(z) J_{mB}\left(mB \frac{z}{z^*}\right) dz \tag{8}$$

where $S(z)$ is used generically to denote the source strength at radial station z. The assumptions made imply that any mB dependence of $S(z)$ can be factored out of the integral and that mB appears only in the argument and order of the Bessel function. It is essential now to recognize that the argument and order of the Bessel function are large and comparable.

Now for $z < z^*$ and $mB >> 1$, the Bessel function is exponentially small. On the other hand, for $z > z^*$ and $mB >> 1$ we have the asymptotic approximation[13]

$$J_{mB}(mB \sec\lambda) \sim \left(\frac{2}{\pi mB \tan\lambda}\right)^{1/2} \cos(mB \tan\lambda - mB\lambda - \pi/4) \tag{9}$$

where $\sec\lambda = z/z^*$, showing that the Bessel function now oscillates rapidly with slowly changing amplitude. The integral in Eq. (8) will therefore be dominated by contributions from the region around $z = z^*$, those from $z < z^*$ being suppressed by the exponential smallness of the Bessel function, those from $z > z^*$ being almost self-canceling because of the rapid oscillations. Consequently, we can make the approximation

$$P_m \sim S(z^*) \int_0^{\infty} J_{mB}\left(mB \frac{z}{z^*}\right) dz \tag{10}$$

where the source strength is evaluated at $z = z^*$ and the lower and upper limits of integration have been extended to zero and infinity, respectively, consistent with the leading-order dominance of the Mach radius region. The integral can be evaluated[13] to give

$$P_m \sim S(z^*) \frac{z^*}{|mB|} \tag{11}$$

(We note that, for helicopter rotors, Hawkings and Lowson[8] used stationary phase techniques to simplify the integration over the blade surface for high values of mB. They also found that the Mach radius provided the dominant contribution to the radiated sound field.)

Interpretation of this result is most important. If, for given θ, there exists a section $z = z^*$ on the blade for which the Mach number component $M_x \cos\theta + zM_t \sin\theta$ is unity, then the radiation in direction θ is dominated by contributions from the immediate vicinity of $z = z^*$ rather than the tip. If $S(z)$ is independent of mB, then the decay of those contributions from the Mach radius is as $|mB|^{-1}$, and the harmonic series converges to a function with logarithmic singularities in the time domain. However, we see from the definition of k_y in the Nomenclature that the loading component of $S(z)$ increases as mB, in which case the harmonic series represents a waveform containing (pole) singularities of order 1. For the thickness component, from the definition of k_x in the Nomenclature, $S(z)$ increases as $(mB)^2$, so that the harmonic series represents a waveform containing (pole) singularities of order 2. (A detailed discussion of the harmonic series results is given in the Appendix. Taking account of the finite chordwise dimension reduces the order of these singularities, as will be shown shortly.) It is thus seen that the present spectral approach is able, quite naturally, to pick up distinctive features characteristic of the time waveform—such as singularities—whenever these exist. Any power law decay with m gives a singularity in some derivative of $p(t)$, whereas if P_m vanishes faster than any inverse power of m, $p(t)$ is infinitely differentiable—and has no special character.

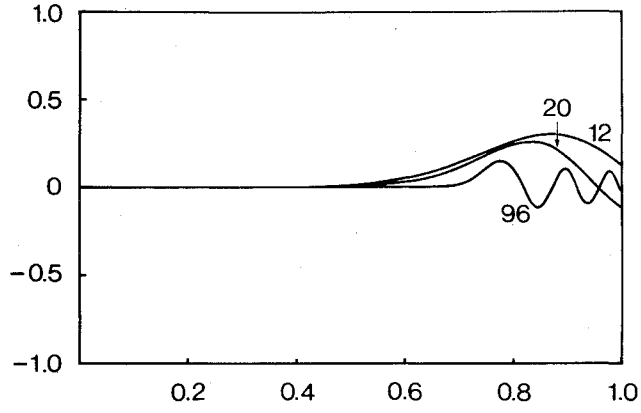

Fig. 2 Plots of the Bessel function $J_{mB}(mBz/z^*)$ as a function of z, $0 \le z \le 1$, with Mach radius $z^* = 0.75$, and with $mB = 12$, 20, and 96 as indicated.

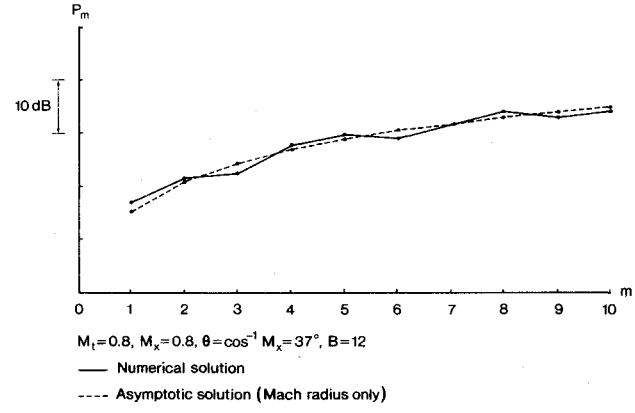

Fig. 3 The harmonic amplitude $|P_m|$ as a function of m for a 12-bladed propeller with $S(z)$ = const; full line, numerical evaluation of Eq. (1); dashed line, Eq. (11); axial Mach number $M_x = 0.8$, tip rotational Mach number $M_t = 0.8$, radiation angle $\theta = \cos^{-1} M_x = 37$ deg.

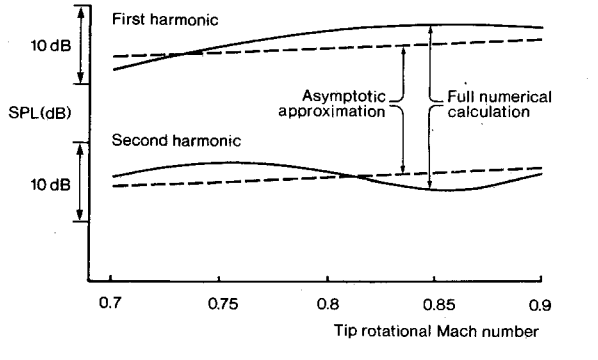

Fig. 4 Comparisons between full numerical evaluation of Eq. (1) and the asymptotic prediction of Eq. (11) (absolute levels) for a supersonic propeller with 12 straight blades, flight Mach number $M_x = 0.8$, emission angle $\theta = \cos^{-1} M_x$.

The result in Eq. (11) can be proved rigorously by standard techniques of analysis and also by stationary phase methods [by writing the integral in Eq. (1) as a double integral over the propeller disk], as was indeed done by Hawkings and Lowson[8] in a restricted case. It might be thought that Eq. (11) would hold only for very large values of mB because the underlying arguments seem to hold only when mB is very large indeed. Take, for example, $z^* = 0.75$ (corresponding, say, to $M_x = 0.8$, $M_t = 0.8$, and $\theta = 37$ deg, which is close to the peak radiation angle for these conditions); then as can be seen from Fig. 2, although it is clear that contributions from regions inboard of the Mach radius are heavily suppressed by the Bessel function, it is not clear that contributions from the outboard region effectively cancel each other even for mB as large as 96. However, it is well known from a vast fund of experience with asymptotics that the end result, Eq. (11), may actually be useful over a much larger range of mB and that the range of validity of an asymptotic expression can only be ascertained through comparisons with the exact results. In this case the comparisons are made in Figs. 3 and 4, where the "exact results" are obtained from numerical evaluation of Eq. (1), with careful use of standard IMSL or NAG routines for evaluation of the Bessel function and the integration itself. In both figures, the spanwise source function $S(z)$ has been taken as constant, a choice that tests Eq. (11) severely, because the next term in the asymptotic development, after the Mach-radius term given in Eq. (11), comes from the tip (as will be shown in a companion paper on higher-order corrections in the asymptotic theory) and naturally has a much larger value when $S(z)$ is constant out to the tip than when $S(z)$ drops (say parabolically) to zero at the tip, as it would for both loading and thickness distributions.

In Fig. 3 we take $M_t = M_x = 0.8$, $\theta = \cos^{-1} M_x = 37$ deg, and $B = 12$, and plot P_m as a function of mB from $mB = 12$ to $mB = 120$. Equation (11) is seen to be quite accurate, and indeed uniformly accurate, over the whole range. The small oscillations are associated with the tip effect that one can expect, on the basis of Eq. (9), to be proportional to $\cos(0.16mB + \alpha_0)$ for some constant α_0. Just such oscillations are seen in Figs. 3 and 4 and will be accounted for in a formula to be given in the companion paper. In Fig. 4 we take $M_x = 0.8$, $\theta = \cos^{-1} M_x = 37$ deg again, but now we plot P_m against tip rotational Mach number M_t, for a 12-bladed propeller and for $m = 1,2$. Again, the leading-order Mach radius contribution Eq. (11) is seen to provide the dominant radiated field, with sinusoidally varying perturbations, of relative order $(mB)^{-1/2}$ if $S(z)$ is constant near the tip, from the tip. Note that the angle $\theta = \cos^{-1} M_x$ chosen for these tests is close to the peak radiation angle.

III. Chordwise Noncompactness Effects

When the chordwise wave number k_x exceeds unity, the effects of chordwise noncompactness become significant. These effects will be most important at high forward speeds, where the Doppler factor can produce a considerable increase in k_x.

From Eqs. (5) and (6), and the definitions in the Nomenclature, we see that noncompactness at each radial station z can be represented by the factor

$$\Psi = \int_{-\infty}^{\infty} f(X)[H(X + \tfrac{1}{2}) - H(X - \tfrac{1}{2})]e^{-ik_x X}\,dX \qquad (12)$$

where $f(X)$ is a general chordwise shape function corresponding either to $F(X)$ (blade loading) or $h(X)$ (blade thickness), and H is the Heaviside unit function. Since the shape functions are always of algebraic form in the region of the blade leading (L) and trailing (T) edges we can put

$$\left.\begin{aligned} f(X) &\sim \alpha_L(\tfrac{1}{2} + X)^{\nu_L} \quad \text{as } X \to -\tfrac{1}{2} \\ f(X) &\sim \alpha_T(\tfrac{1}{2} - X)^{\nu_T} \quad \text{as } X \to \tfrac{1}{2} \end{aligned}\right\} \qquad (13)$$

An integrable singularity in the leading-edge loading can, as usual, be tolerated, corresponding to $-1 < \nu_L < 0$.

As in previous sections, mB is assumed to be large so that k_x is also large. We can then evaluate Eq. (12) asymptotically, using the methods outlined in Chap. 4 of Lighthill,[14] leading to

$$\Psi \sim \frac{\alpha_L \nu_L! \exp[\pm i|k_x|/2 \mp i(\nu_L + 1)\pi/2]}{|k_x|^{\nu_L+1}} + \frac{\alpha_T \nu_T! \exp[\mp i|k_x|/2 \pm i(\nu_T + 1)\pi/2]}{|k_x|^{\nu_T+1}} \qquad (14)$$

where the upper or lower signs are used according as m, the harmonic index, is positive or negative. Consider first the case $\nu_L < \nu_T$, where the shape function $f(X)$ is weighted toward the leading edge. The first term in Eq. (14) is then dominant. Second, when the chordwise shape function is symmetric we have

$$\alpha_L = \alpha_T = \alpha, \qquad \nu_L = \nu_T = \nu$$

say, and Eq. (14) reduces to

$$\Psi \sim \frac{2\alpha\nu!}{|k_x|^{\nu+1}} \cos\left[\frac{|k_x|}{2} - (\nu + 1)\frac{\pi}{2}\right] \tag{15}$$

In this case the noise level will oscillate as k_x is increased, and the envelope of the oscillations will reduce as $|k_x|^{-\nu-1}$. The two results, Eqs. (14) and (15), provide a simple description and explanation of the results found by Hanson[15] (see, in particular, his Fig. 9) who examined (numerically) three types of chordwise shape function for loading noise. Of these, two were leading-edge dominated and had almost identical monotonic algebraic decay of Ψ with increasing k_x, differing only in a constant corresponding to different values of α_L, the distributions elsewhere over the chord being irrelevant. The third was essentially symmetric about the midchord and gave oscillatory behavior in Ψ due to correlated comparable leading- and trailing-edge effects, with algebraic envelope decay similar to that of the first two.

The importance of expressions Eqs. (14) and (15) is that 1) they show how noncompactness effects at each station are dominated by leading- or trailing-edge behavior, and 2) they form a basis for subsequent evaluation of the spanwise integral that is needed to determine the overall acoustic benefit of noncompactness. This overall benefit cannot necessarily be assessed by examining a single blade section (as was done in Fig. 9 of Hanson[15]).

Assume now that the noncompactness factor is given asymptotically by the first term in Eq. (14), i.e., the shape function $f(X)$ is weighted toward the leading edge. Then, from Eqs. (1) and (14),

$$P_m \sim \alpha_L \nu_L! \exp\left[\mp i(\nu_L + 1)\frac{\pi}{2}\right] \times \int_{z_0}^{1} \frac{S(z)}{|k_x|^{\nu_L+1}} J_{mB}\left(mB\frac{z}{z^*}\right) e^{\pm i|k_x|/2}\, dz \tag{16}$$

where $S(z)$ is now understood no longer to contain the noncompactness factor Ψ. The form of the integral in Eq. (16) is similar to that in Eq. (8) except that now there is another rapidly varying function of mB in the noncompactness phase term. This leads to considerable complications in general, and these will be dealt with in a separate paper on all such spanwise interference effects. However, we can get a result that gives a first estimate of the (very strong) effects of noncompactness by assuming k_x to be approximately constant with radius; then we can proceed as before and arrive at

$$P_m \sim \frac{\alpha_L \nu_L! S(z^*) z^*}{|mB|\,|k_x^*|^{\nu_L+1}} \exp\left[\mp i(\nu_L + 1)\frac{\pi}{2} \pm \frac{i|k_x^*|}{2}\right] \tag{17}$$

where k_x^* is the value of k_x at $z = z^*$. For k_x to be constant with radius we are assuming, essentially, that the projection of the chord onto a line parallel to the engine axis is constant with radius. There are thus no spanwise interference effects; such effects are actually analogous to those of sweep.

Equation (17) is superficially similar to Eq. (11) that, we observed, indicated the production of logarithmic singularities (or worse). However, taking into account the dependence of $S(z)$ and k_x on mB, we find that Eq. (17) decays as $\mathrm{sgn}(mB)|mB|^{-\nu_L-1}$ for the loading component of the sound field and as $|mB|^{-\nu_L}$ for the thickness component. (The actual dependence on mB is more complex than this; a full description of the harmonic components and the associated waveforms is given in the Appendix.) Consider first three types of loading distribution. When there is an integrable singularity in the leading-edge loading ($-1 < \nu_L < 0$), there are weak algebraic singularities in the waveform; when the leading-edge loading is finite ($\nu_L = 0$), logarithmic singularities are generated; and when the leading-edge loading is zero ($\nu_L > 0$), there are no singularities generated (though there are singularities in some derivative of the pressure).

Consider next thickness noise, where the harmonic decay is controlled by the shape of the leading edge. For a blunt leading edge ($0 < \nu_L < 1$), there are weak algebraic singularities in the waveform; for a wedge-shaped leading edge ($\nu_L = 1$), logarithmic singularities are generated; and for a cusp-shaped leading edge ($\nu_L > 1$), there are no singularities in the waveform. The results for thickness noise in the case of a blunt leading edge agree with those obtained previously by Tam[10] and Chapman[11] and in the case of a wedge-shaped leading edge with those obtained by Amiet.[12]

It is interesting to note the variations with tip rotational Mach number M_t. Here we must take account, through Eq. (9), of the variation of z^* with M_t, and we must note that if M_x and θ are fixed, then as M_t varies, the section relative Mach number M_r^* at the Mach radius also stays fixed. For loading noise we find $P_m \sim M_t^{-\nu_L-1}$. Since, for loading, ν_L is always greater than -1, this means that P_m is a *decreasing function* of M_t. For thickness noise we find $P_m \sim M_t^{-\nu_L}$. Since, for blade thickness, ν_L is always greater than 0, this shows again that P_m is a decreasing function of M_t. This *algebraic decrease* contrasts markedly with the *exponential increase* at subsonic tip speeds that was discussed in Part I. Note that it is essential to incorporate chordwise noncompactness effects if the decrease of P_m with increase of M_t is to be predicted.

In Fig. 5 a comparison is shown between a full numerical calculation and the asymptotic approximation Eq. (17) for a 12-bladed propeller of constant chord. The plot shows the reduction in the thickness noise component due to noncompactness for the first two harmonics of blade passing frequency. The values of α_L and ν_L were determined from the form of the full chordwise shape function in the region of the leading edge. The shape function was chosen so that $\nu_L = 1$ and $\nu_T = 2$. From Fig. 5 it can be seen that the asymptotic approximation agrees quite well with the full numerical cal-

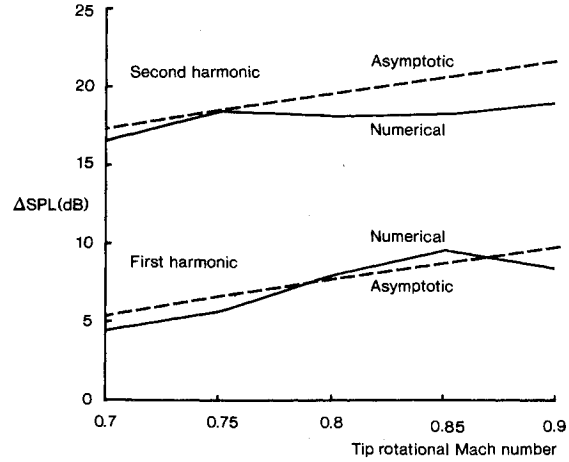

Fig. 5 Comparisons between the full numerical evaluation of Eq. (1) and the asymptotic prediction of Eq. (17) for the effects of chordwise noncompactness. The ordinate refers to the difference Δ between the compact-chord case [$\Psi \equiv 1$ in Eqs. (3) and (4)] and the actual finite-chord case. The propeller has 12 straight blades, the flight Mach number is $M_x = 0.8$, and the emission angle is $\theta = \cos^{-1} M_x$.

culation over the range of tip speeds examined. At second harmonic, there is very close agreement between the two calculations at the lower tip speeds but some discrepancy at higher tip speeds. Since the approximate calculation is asymptotic in mB, we would generally except the results at second harmonic to be *more* accurate than those at first. However, in deriving Eq. (17), we assumed k_x to be approximately constant with z, and we find that, for a propeller of *constant chord*,

$$\frac{\mathrm{d}}{\mathrm{d}z}\left(\frac{k_x}{2}\right) = -\frac{mBM_t^3 zc/D}{(1 - M_x\cos\theta)M_r^3}$$

At first harmonic, for the case under consideration, $(\mathrm{d}/\mathrm{d}z)(k_x/2)$ is less than 1 for the range of tip speeds examined, indicating that, to a first approximation, the variations in phase along the blade span can be neglected. This is confirmed by the agreement between the asymptotic and numerical predictions in Fig. 5. However, at higher harmonics the phase variations along the blade span will be significant and the asymptotic approximation Eq. (17) will be inaccurate, particularly at high tip speeds, and this is evident in the second harmonic results in Fig. 5.

To improve on the local result in Eq. (11), or the global result in Eq. (17) incorporating noncompactness in the special case k_x = const, we have to return to the integral Eq. (16) and properly account for the competition between spanwise interference effects associated with chordwise noncompactness and the basic radiation efficiency Bessel function factor. This can be done, but the results will be presented elsewhere because one can at the same time include the effects of blade sweep, which are very similar to those of noncompactness and which are sufficiently important (and novel) that they call for more detailed analysis than can be given here.

IV. Concluding Remarks

The essential point of this paper has been the identification of the Mach radius as the dominant source of supersonic propeller noise, and the derivation of Eq. (11) for the Mach radius radiation. This formula governs the acoustic field in and ahead of the rotor plane up to the angle for which the Mach radius coincides with the blade tip. Further ahead, the radiation is essentially of subsonic type, is dominated by the blade tips, and is described by the subsonic radiation expressions of Part I. Good agreement has been found between the asymptotic prediction and the results of full numerical evaluation of the radiation integrals. The transition between subsonic and supersonic radiation, as z^* moves through the tip value 1, will be given in a companion paper on higher-order approximations of the large-B theory.

A first approximation has been given here to effects of chordwise noncompactness on supersonic propeller noise. These effects indicate that as tip Mach number increases, the harmonic components of the radiation increase exponentially in the subsonic range but decrease algebraically for Mach-radius radiation. Inspection of the variation of the Fourier components of large order m indicates (see Appendix) that singularities are produced on certain surfaces in the field, and the singular nature of the pressure has been obtained, for both thickness and loading noise, and with inclusion of forward (axial) Mach number effects. These results are general and complete, although they are only sketched briefly in the Appendix, and include a number of results previously published and relating to restricted conditions.

One point should be stressed with regard to the Mach radius. In general, the Mach radius and sonic radius (defined by $M_r = 1$) will not coincide, and therefore in general transonic aerodynamic codes will not be needed to provide the loading input to Eq. (11).

Appendix: Harmonic Series and Pressure Waveforms for Straight-Bladed Supersonic Propellers

On suppressing constant factors we find that the waveform generated by a straight-bladed propeller operating at supersonic conditions, when noncompactness effects are also suppressed for the present, is of the form

$$p(t) \sim \frac{S(z^*)}{|mB|} \times \sum_{m=-\infty}^{\infty} \exp\left\{imB\left[\frac{\Omega(t - r_0/c_0)}{(1 - M_x\cos\theta)} + \frac{\pi}{2} - \psi_0\right]\right\} \tag{A1}$$

We now consider three cases: first, $S(z^*)$ independent of mB; second, corresponding to steady loading noise, $S(z^*) \sim mB$; third, corresponding to thickness noise, $S(z^*) \sim (mB)^2$.

Define the function

$$F(\xi) = B^\eta \xi^\eta \mathrm{sgn}(\xi)\exp[i\xi B(\Omega_D\tau + \alpha)] \tag{A2}$$

where Ω_D represents the Doppler shifted angular frequency $\Omega/(1 - M_x\cos\theta)$, τ the retarded time $(t - r_0/c_0)$, and $\alpha = \pi/2 - \psi_0$. The parameter η can take the values -1, 0, and $+1$ corresponding, respectively, to the three cases above.

The Fourier transforms are, in the notation of Lighthill,[14]

$$G(\chi) = \int_{-\infty}^{\infty} F(\xi)\exp(-i2\pi\xi\chi)\,\mathrm{d}\xi \tag{A3}$$

$$= \frac{-2}{B}\,\mathscr{H}\left|\Omega_D\tau + \alpha - \frac{2\pi\chi}{B}\right|, \quad \eta = -1 \tag{A4}$$

$$= \frac{2i}{B}\left(\Omega_D\tau + \alpha - \frac{2\pi\chi}{B}\right)^{-1}, \quad \eta = 0 \tag{A5}$$

$$= \frac{-2}{B}\left(\Omega_D\tau + \alpha - \frac{2\pi\chi}{B}\right)^{-2}, \quad \eta = +1 \tag{A6}$$

Now use Poisson's summation formula (Theorem 28 in Lighthill[14])

$$\sum_{m=-\infty}^{\infty} F(m) = \sum_{n=-\infty}^{\infty} G(n) \tag{A7}$$

to get the waveforms generated in the three cases as

$$p(t) \sim \frac{-2}{B}\sum_{n=-\infty}^{\infty}\mathscr{H}\left|\Omega_D\tau + \alpha - \frac{2\pi n}{B}\right|, \quad \eta = -1 \tag{A8}$$

$$\sim \frac{2i}{B}\sum_{n=-\infty}^{\infty}\left(\Omega_D\tau + \alpha - \frac{2\pi n}{B}\right)^{-1}, \quad \eta = 0 \tag{A9}$$

$$\sim \frac{-2}{B}\sum_{n=-\infty}^{\infty}\left(\Omega_D\tau + \alpha - \frac{2\pi n}{B}\right)^{-2}, \quad \eta = +1 \tag{A10}$$

In each case, each of the summed singularities corresponds to the passage of a blade.

If we include noncompactness effects then, on suppressing constant factors, we can write the acoustic waveform as

$$p(t) \sim \sum_{m=-\infty}^{\infty}\frac{S(z^*)}{|mB|^{\nu_L+2}}\exp\left[imB(\Omega_D\tau + \alpha^*) - i(\nu_L + 1)\frac{\pi}{2}\mathrm{sgn}(m)\right] \tag{A11}$$

where $\alpha^* = k_x^*/2mB + \pi/2 - \psi_0$.

For the loading noise source with $-1 < \nu_L < 0$, define the function

$$F(\xi) = \left\{\cos\left[(\nu_L + 1)\frac{\pi}{2}\right] - \operatorname{sgn}(\xi)\sin\left[(\nu_L + 1)\frac{\pi}{2}\right]\right\}|\xi|^{-\nu_L - 1}\operatorname{sgn}(\xi)e^{i\xi B(\Omega_D\tau + \alpha^*)} \tag{A12}$$

then proceed as above to obtain

$$p(t) \sim -2i(-\nu_L - 1)!B^{\nu_L}\sum_{m=-\infty}^{\infty}|\Omega_D\tau + \alpha^* - 2\pi m/B|^{\nu_L} \times \left\{\sin\left(\frac{\nu_L\pi}{2}\right)\cos\left[(\nu_L + 1)\frac{\pi}{2}\right]\operatorname{sgn}\left(\Omega_D\tau + \alpha^* - \frac{2\pi m}{B}\right) + \sin\left[(\nu_L + 1)\frac{\pi}{2}\right]\cos\left(\frac{\nu_L\pi}{2}\right)\right\} \tag{A13}$$

The waveform thus contains weak algebraic singularities. Similar analyses for $\nu_L = 0$ and $\nu_L = 1$ produce the waveforms

$$p(t) \sim 2i\sum_{m=-\infty}^{\infty}\mathcal{H}\left|\Omega_D\tau + \alpha^* - \frac{2\pi m}{B}\right| \tag{A14}$$

$$p(t) \sim 2iB\sum_{m=-\infty}^{\infty}\left(\Omega_D\tau + \alpha^* - \frac{2\pi m}{B}\right)\left[\mathcal{H}\left(\frac{B}{2\pi}\right) + \mathcal{H}\left|\Omega_D\tau + \alpha^* - \frac{2\pi m}{B}\right|\right] \tag{A15}$$

respectively. The waveform in Eq. (A14), which is generated by a loading function finite at the leading edge, contains periodic logarithmic singularities. In Eq. (A15), representing the waveform generated by a loading function that is zero at the leading edge, the singularities have effectively been removed.

For the thickness noise source define

$$G(\xi) = \left\{\cos\left[(\nu_L + 1)\frac{\pi}{2}\right] - i\operatorname{sgn}(\xi)\sin\left[(\nu_L + 1)\frac{\pi}{2}\right]\right\}|\xi|^{-\nu_L}e^{i\xi B(\Omega_D\tau + \alpha^*)} \tag{A16}$$

and then, for $0 < \nu_L < 1$ (airfoil with a blunt leading edge), we obtain the waveform

$$p(t) \sim 2(-\nu_L)!B^{\nu_L - 1}\sum_{m=-\infty}^{\infty}\left|\Omega_D\tau + \alpha^* - \frac{2\pi m}{B}\right|^{\nu_L - 1} \times \left\{\cos\left[(1 + \nu_L)\frac{\pi}{2}\right]\cos\left[(1 - \nu_L)\frac{\pi}{2}\right] + \sin\left[(1 + \nu_L)\frac{\pi}{2}\right]\sin\left[(1 - \nu_L)\frac{\pi}{2}\right] \times \operatorname{sgn}\left(\Omega_D\tau + \alpha^* - \frac{2\pi m}{B}\right)\right\} \tag{A17}$$

which is of the same form as Eq. (A13) and contains weak algebraic singularities. For $\nu_L = 1$ (airfoil with a wedge-shaped leading edge), we obtain

$$p(t) \sim 2\sum_{m=-\infty}^{\infty}\mathcal{H}\left|\Omega_D\tau + \alpha^* - \frac{2\pi m}{B}\right| \tag{A18}$$

which is, basically, identical to Eq. (A14) and contains logarithmic singularities. For $\nu_L > 1$, corresponding to an airfoil with a cusp-shaped leading edge, the waveform is given by Eq. (A17) which, since $\nu_L - 1 > 0$, now contains no singularities or discontinuities (except in pressure derivatives).

Acknowledgments

Some of this work was carried out while the second author was Principal Engineer, Rolls-Royce plc, Derby, England. The work was also supported by the Science and Engineering Research Council, U.K., and is published by permission of the Directors of Rolls-Royce plc.

References

[1]Parry, A. B., and Crighton, D. G., "Asymptotic Theory of Propeller Noise—Part I: Subsonic Single-Rotation Propeller," *AIAA Journal*, Vol. 27, No. 9, 1989, pp. 1184–1190.

[2]Hanson, D. B., "Helicoidal Surface Theory for Harmonic Noise of Propellers in the Far Field," *AIAA Journal*, Vol. 18, No. 10, 1980, pp. 1213–1220.

[3]Hanson, D. B., "Near Field Noise of High Speed Propellers in Forward Flight," AIAA Paper 76-0565, July 1976.

[4]Farassat, F., "Production of Advanced Propeller Noise in the Time Domain," *AIAA Journal*, Vol. 24, No. 4, 1986, pp. 578–584.

[5]Schmitz, F. H., and Yu, H., "Helicopter Impulsive Noise: Theoretical and Experimental Status," *Journal of Sound and Vibration*, Vol. 109, Sept. 1986, pp. 361–422.

[6]Lindblad, I., "Asymptotic Analysis of the Transonic Region of a High-Speed Propeller," AIAA Paper 89-1077, April 1989.

[7]Diprose, K. V., "Some Propeller Noise Calculations Showing the Effect of Thickness and Planform," Royal Aircraft Establishment, Farnborough, England, Tech. Note MS 19, 1955.

[8]Hawkings, D. L., and Lowson, M. V., "Theory of Open Supersonic Rotor Noise," *Journal of Sound and Vibration*, Vol. 36, Sept. 1974, pp. 1–20.

[9]Ffowcs Williams, J. E., and Hawkings, D. L., "Sound Generation by Turbulence and Surfaces in Arbitrary Motion," *Philosophical Transactions of the Royal Society of London*, Series A: Mathematical and Physical Sciences, Vol. 264, May 1969, pp. 321–342.

[10]Tam, C. K. W., "On Linear Acoustic Solutions of High Speed Helicopter Impulsive Noise Problems," *Journal of Sound and Vibration*, Vol. 89, July 1983, pp. 119–134.

[11]Chapman, C. J., "Shocks and Singularities in the Pressure Field of a Supersonically Rotating Propeller," *Journal of Fluid Mechanics*, Vol. 192, July 1988, pp. 1–16.

[12]Amiet, R. K., "Thickness Noise of a Propeller and its Relation to Blade Sweep," *Journal of Fluid Mechanics*, Vol. 192, July 1988, pp. 535–560.

[13]Abramowitz, M., and Stegun, I. A., *Handbook of Mathematical Functions*, Dover, New York, 1965.

[14]Lighthill, M. J., *An Introduction to Fourier Analysis and Generalised Functions*, Cambridge Univ. Press, Cambridge, England, 1958.

[15]Hanson, D. B., "Influence of Propeller Design Parameters on Far Field Harmonic Noise in Forward Flight," *AIAA Journal*, Vol. 18, No. 11, 1980, pp. 1313–1319.